

## Electrochemical Behaviour of Hafnium in Anhydrous *n*-butanol Containing Tetraethylammonium Bromide

Changhong Wang, Shenghai Yang\*, Yongming Chen, Xiyun Yang, Biao Wang, Jing He, Chaobo Tang

School of Metallurgy and Environment, Central South University, Changsha 410083, China

\*E-mail: [Yangshcsu@163.com](mailto:Yangshcsu@163.com)

Received: 5 July 2016 / Accepted: 24 October 2016 / Published: 12 December 2016

---

The electrochemical behavior of hafnium in Et<sub>4</sub>NBr anhydrous *n*-butanol solutions were investigated using electrochemical measurements, ICP-AES and SEM techniques. Results revealed that the open circuit potential gets more positive owing to the increased passivity of a barrier HfO<sub>2</sub> layer with increasing immersion time until a steady state value is reached. Cyclic voltammetry did not present an anodic active dissolution section near corrosion potential as a result of the formation of the oxide layer, which was followed with severe pitting corrosion. SEM images confirmed the existence of pits on the electrode surface. ICP-AES method of chemical analysis demonstrated that the rate of pitting corrosion of Hf increased with increasing applied anodic potential. The pitting potential ( $E_{\text{pit}}$ ) and the repassivation potential ( $E_{\text{p}}$ ) can be determined jointly by cyclic voltammetry and galvanostatic measurements.  $E_{\text{pit}}$  increased with boosting potential scanning rate but decreased with enhancing solution temperature. The incubation time was necessary for pit growth. The impedance spectra showed two time constants at various potentials applied, and the passive layer resistance declined with an increase in potential.

---

**Keywords:** Hafnium; anhydrous *n*-butanol; Electrochemical; Cyclic voltammetry; electrochemical impedance spectra; Pitting corrosion

### 1. INTRODUCTION

Hafnium alkoxide is mainly used for the deposition of hafnium oxide(HfO<sub>2</sub>) layers by atomic layer deposition (ALD), and deposited in this manner, the hafnium-based high-*k* dielectrics present much more stable electrical characteristics compared with the ones formed by chemical vapors or sputtering [1]. With the rapid development of semiconductor industry, a gate dielectric thickness in the field effect transistor (FET) closely approached its physical limits as a result of a rise in leakage currents owing to tunneling effects [2-4]. Therefore, it is necessary to replace the SiO<sub>2</sub> with a high-*k*

gate dielectric.  $\text{HfO}_2$  layers are among the most promising high- $k$  dielectrics candidates to meet the standard for substituting the traditional  $\text{SiO}_2$  gate oxide in semiconductor devices [4-5].

Due to the particularity of metal hafnium, it fails to produce hafnium alkoxide when hafnium or hafnium oxide directly react with alcohol. At present, the mainstream method of producing hafnium alkoxides is on the base of the halide synthesis [6]. The approach for preparing  $\text{Hf}(\text{OR})_4$  has such disadvantages as a long process, poor working conditions, high cost, and low efficiency [7]. Based on these, the direct electrochemical synthesis of metal alkoxides by the sacrifice of metals anode in anhydrous alcohols containing a conductive admixture is expected to be a quite promising approach. This electrochemical synthesis seems promising for the direct conversion of the less electropositive metals to their alkoxides due to its simplicity and high productivity as well as its continuous and non-polluting character (with hydrogen as the major by-product) [6]. In our earlier works, we have prepared several niobium and tantalum alkoxides by electrochemical process [8-10]. In 1995, Hafnium  $n$ -butoxide was obtained for the first time by Turevskaya et al. [11] with the electrochemical method involving electrolysis of an  $n$ -butanol solution containing tetraethylammonium bromide with a platinum cathode and a hafnium anode. Hafnium  $n$ -butoxide compared to hafnium ethoxide is liquid at room temperature which seems to be more favorable for the deposition of hafnium oxide ( $\text{HfO}_2$ ) layers by atomic layer deposition (ALD). However, the electrochemical behaviors of this process have not been investigated so far.

Hafnium is a valve metal and some literature has been reported on its electrochemistry in aqueous solutions [12-17]. Bartels et al. [12] studied the growth of  $\text{HfO}_2$  film on the anode surface in various solutions, including alkaline, neutral and acidic electrolytes, and drew a conclusion that Hf in acidic electrolytes suffered from severe localized corrosion after the anodic breakdown of the oxides. Most investigations were related with the formation of anodic oxide films and the kinetics of dissolution of these films [12, 16, 17]. Titanium and tantalum, which are close to hafnium in its properties, were investigated in anhydrous alcohols, and the results indicated that they could suffer from severe localized corrosion [18-19].

Despite some study on the electrochemistry of Hf in aqueous solutions, only one [20] literature reported on the electrochemical behaviors of hafnium in anhydrous ethanol. In our paper, the electrochemical behavior of hafnium was studied in anhydrous  $n$ -butanol containing  $\text{Et}_4\text{NBr}$ , by means of various electrochemical measurement techniques including open circuit potential measurements, potentiodynamic anodic polarization, cyclic voltammetry, galvanostatic, potentiostatic and impedance methods. ICP-AES technique of chemical analysis was also applied to confirm results acquired from electrochemical measurements. SEM examinations on the anode surface was also carried out.

## 2. EXPERIMENTAL

$\text{Et}_4\text{NBr}$  was supplied by Sinopharm Chemical Reagent Corporation Limited. Anhydrous  $n$ -butanol was purchased from Tianjing Damao Chemical Reagent Corporation. The working electrode used was provided by the Northwest Institute for Non-ferrous Metal Research, and was made from a

very pure hafnium rod (99.9%). The electrode employed offered an active flat disc shaped surface of 4.28 mm<sup>2</sup> geometric area to contact with test solution.

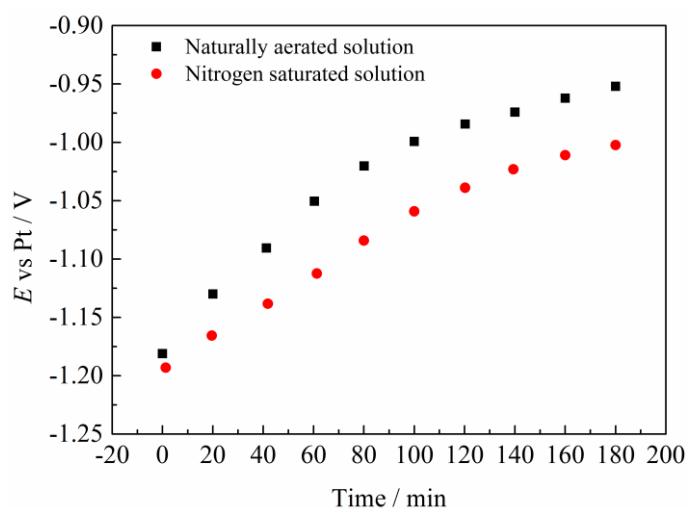
The electrochemical experiments were performed in a 250 mL volume glass electrolytic cell utilizing Pt foils of 1 cm × 1 cm and 2 cm × 2 cm geometric areas as auxiliary and reference electrodes, respectively. The experiments were performed in anhydrous *n*-butanol containing Et<sub>4</sub>NBr of different concentrations (0.02–0.10 M). All chemicals used were of analytical grade. Each experiment was performed in aerated stagnant solutions at the corresponding temperature (±1 °C) kept by a thermostat system. The gases used for studying its effects on the electrode potential of passive Hf in anhydrous *n*-butanol were purified and dried before bubbling in the electrolyte. The gas was bubbled approximately 20 min in the test solution before electrode immersion. Before each run, the sample electrode was consecutively polished with a series of emery papers from a coarse grade of 1000 to fine grade of 3000. The hafnium electrode was then successively rinsed with ethanol and *n*-butanol and finally immersed in the electrolytic cell [20]. When a stable potential value was reached (stable open circuit potential, less than 1.0 mV change over 3 min [21,22]), each measurement was performed.

Electrochemical measurements were conducted by means of a potentiostat/galvanostat (supplied by Shanghai Chenhua Instrument Corporation, CHI660C Electrochemical Workstation) linked to a personal computer. Cyclic voltammetric measurements were performed via scanning the potential linearly from -1 V (Pt) more negative than the open circuit potential ( $E_{ocp}$ ) toward the noble direction at the corresponding scanning rate up to the given value, reversing with the same scanning rate toward the negative direction, and finally returning to the initial potential to form a complete circuit. Potentiodynamic polarization curve measurements were set from -1 V (Pt) more negative than  $E_{ocp}$  up to 3 V (Pt) at a scanning rate of 1 mV s<sup>-1</sup>. Galvanostatic measurements were used at a constant anodic current density upon the Hf electrode, and the variation in potential as a function of time was recorded. EIS measurements were adopted by AC signals of amplitude 5 mV in the frequency range from 0.1 Hz up to 0.1 MHz. All impedance results were fit to suitable equivalent circuits by employing computer program ZSimDemo 3.30d. In potentiostatic current/time transients, a constant anodic potential is applied on the sample surface, and the variation in current as a function of time was recorded.

The morphology observations of the sample surface was achieved by SEM employing a JEOL JSM-6360LV electron microscope. SEM examinations were adopted to analyze the hafnium surface after anodization at different potentials for 5 min in 0.06 M Et<sub>4</sub>NBr anhydrous *n*-butanol solutions: (A) 0.5 V (before  $E_{pit}$ ); (B) 1.8 V (after  $E_{pit}$ ); (C) 2.1 V (after  $E_{pit}$ ); (D) 2.4 V (after  $E_{pit}$ ). The accelerating influence of the applied anodic potential towards pitting corrosion of Hf was evaluated in 0.06 M Br<sup>-</sup> solutions at 30 °C, using an independent chemical method of analysis, namely ICP-AES. The Hf<sup>4+</sup> ions concentration as a function of the potential applied was measured in the aggressive solution after holding the sample for 5.0 min at the given potential. Measurements were carried out by Perkin-Elmer Optima 5300 Dual View inductively coupled plasma-atomic emission spectrometry (ICP-AES) instrument linked to AS 93 Plus autosampler.

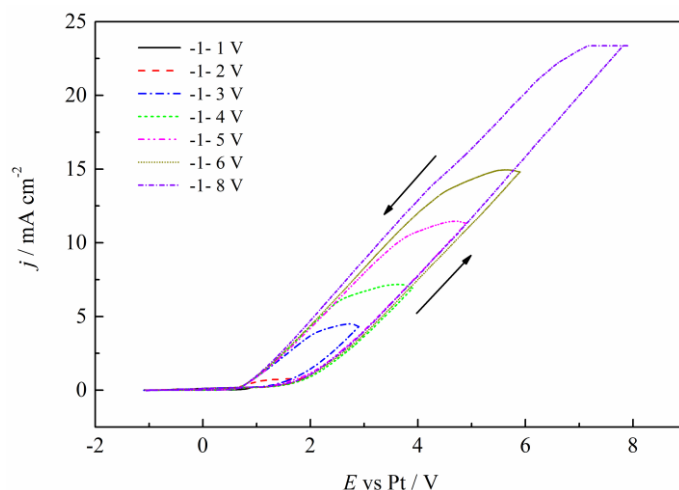
### 3. RESULTS AND DISCUSSION

Fig. 1 presents the influence of the dominating gas on the electrode potential of hafnium in anhydrous *n*-butanol containing 0.06 M Et<sub>4</sub>NBr at 30 °C. It is clear that in both solutions the potential enhances with increasing immersion time until a steady state value in the anhydrous solution (contains less than 1% water) is obtained. This steady state value was considered as the stable open circuit potential. This increase in potential indicated that water, even if in traces, has a great influence on the electrochemical behaviour of hafnium in anhydrous solution, and the Hf surface becomes more passive after longer immersion time in the test solution. The passivation enhances in the presence of air as can be observed from the noble shift in the steady state potential of hafnium in naturally aerated solution compared to the values in nitrogen saturated solutions. As a result, a shift of approximate 50 mV toward the noble direction is observed. These phenomena may be attributed to an increased passive film thickness or increased stoichiometry of the surface oxide film [17].



**Figure 1.** Effect of the dominating gas on the electrode potential of Hf in 0.06 M Et<sub>4</sub>NBr anhydrous *n*-butanol solution at 30 °C.

Fig. 2 presents the cyclic voltammogram of Hf beginning from -1 V (Pt) and reversed at different noble potentials ( $E_{s,a}$ ) in 0.06 M Et<sub>4</sub>NBr anhydrous *n*-butanol solution at 30 °C. It is clearly seen that as  $E_{s,a}$  are made more positive, more pronounced hysteresis loops appear. When  $E_{s,a}$  is reversed at 1 V (Pt), no phenomenon of the hysteresis loop occurs in the corresponding curve, and the maximum current density is only as low as 0.186 mA cm<sup>-2</sup>. While  $E_{s,a}$  is reversed at 2 V (Pt), a rather small cyclic hysteresis loop appears, and the maximum current density rises to 0.825 mA cm<sup>-2</sup>. On the other hand, when  $E_{s,a}$  is reversed at potentials that exceed 3 V (Pt), the shape of the hysteresis loop does not change with  $E_{s,a}$  basically. Based upon both the current density requirement and electrochemical synthesis, it is reasonable to set the reversed potential as 3 V (Pt).



**Figure 2.** Effect of the reversed potentials ( $E_{s,a}$ ) on the cyclic voltammogram of Hf in 0.06 M  $\text{Et}_4\text{NBr}$  *n*-butanol solution beginning from -1 V (Pt) at 30 °C.

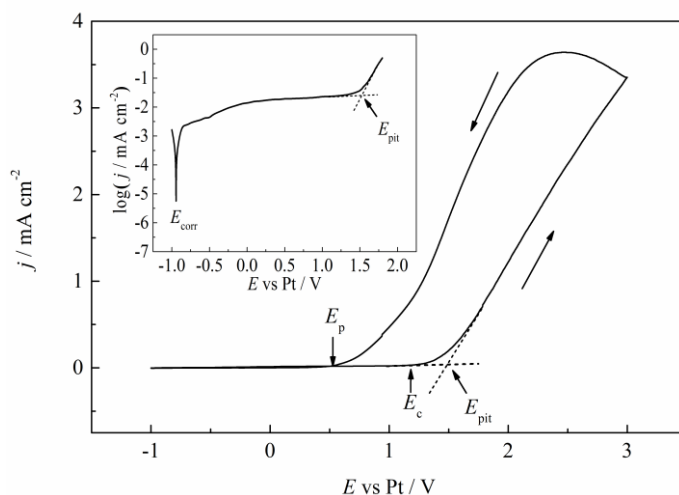


**Figure 3.** Cyclic voltammogram of Hf in 0.06 M  $\text{Et}_4\text{NBr}$  *n*-butanol solution at a scan rate of 1  $\text{mV s}^{-1}$  at 30 °C.

Fig. 3 presents the cyclic voltammogram of Hf beginning from -1 V (Pt) to 3 V (Pt) in 0.06 M  $\text{Et}_4\text{NBr}$  anhydrous *n*-butanol solution at a scanning rate of 1  $\text{mV s}^{-1}$  at 30 °C. It is observed that the anodic scanning region does not present an activation dissolution part near the corrosion potential ( $E_{\text{corr}}$ ) (see the insert of Fig. 3). The lack of active section could be assigned to self-passivation of the sample due to the formation of an  $\text{HfO}_2$  layer on anode surface. This phenomenon demonstrates that the barrier film is stable to contact test solution at and near  $E_{\text{corr}}$ . With increasing potential applied, the passive current density ascends gradually. This rise in current density might be assigned to the chemical dissolution of  $\text{HfO}_2$  by the intense attack of  $\text{Br}^-$  anions after its adsorption and incorporation [23]. Afterwards, the potential rises to a certain value, defined as the critical potential ( $E_c$ ). When the applied potential exceeds  $E_c$ , current density rises slowly until the pitting potential ( $E_{\text{pit}}$ , roughly estimated as shown in Fig. 3) is reached. The value of  $E_{\text{pit}}$  is taken as a measure to evaluate the

resistance of the testing materials towards pitting corrosion. As the anodic potential exceeds  $E_{\text{pit}}$ , the current density shows to go up abruptly and nearly linearly, without the appearance of oxygen evolution, which corresponds to the puncture of the passivated film and the initiation and propagation of pitting corrosion.

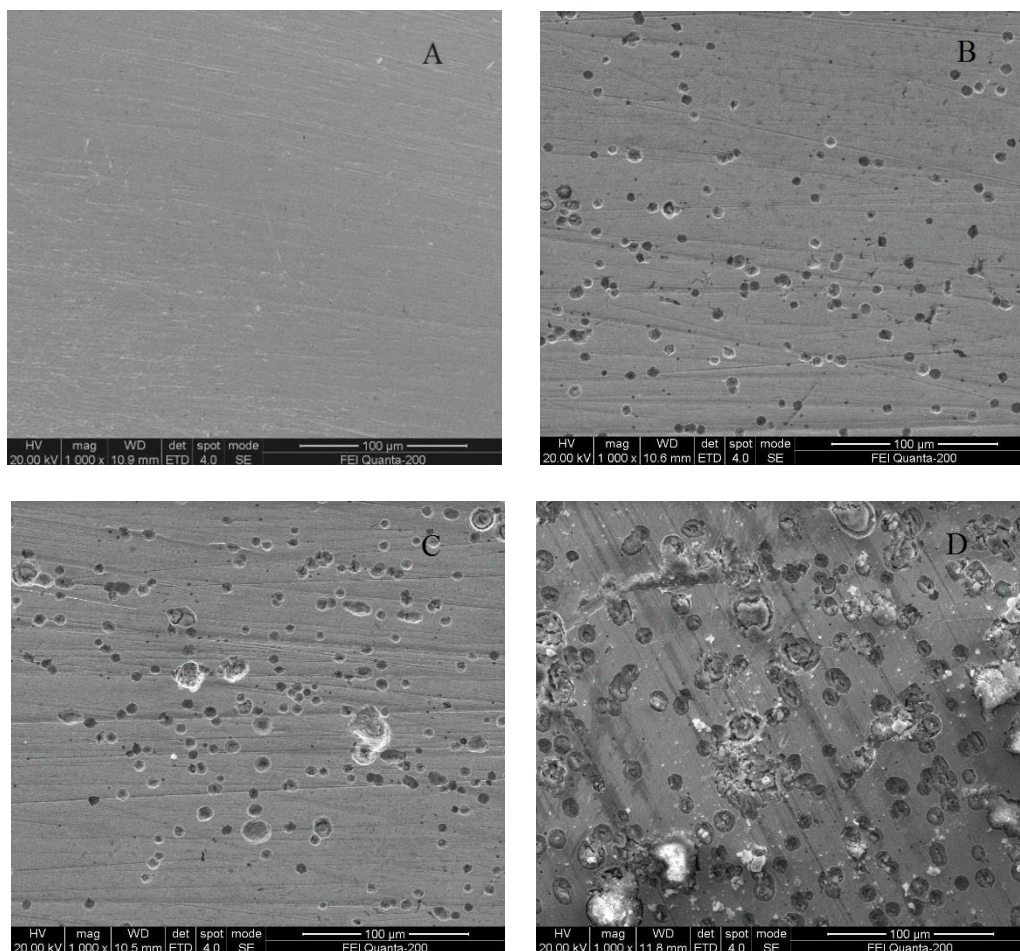


**Figure 4.** SEM observations of Hf surface after anodization at different potentials for 5 min in 0.06 M Et<sub>4</sub>NBr anhydrous *n*-butanol solutions: (A) 0.5 V (before  $E_{\text{pit}}$ ); (B) 1.8 V (after  $E_{\text{pit}}$ ); (C) 2.1 V (after  $E_{\text{pit}}$ ); (D) 2.4 V (after  $E_{\text{pit}}$ ).

Fig. 4 shows SEM observations of the Hf surface after anodization for 5.0 min at different potentials in anhydrous *n*-butanol. As illustrated in Fig. 4, no signs of pitting corrosion appear on the sample applied by an anodic potential negative to  $E_{\text{pit}}$  (image A). On the other hand, SEM observation presents severe pitting corrosion on electrode surface (positive to  $E_{\text{pit}}$ , images B, C and D). This enhancement in potential leads to the deeper and more irregular holes. It is commonly accepted that corrosion of hafnium takes place via pitting rather than uniform corrosion [12]. This behaviour can be explained in terms of the natural quick formation of a stable and electrically insulating inert passivated oxide film. The Br<sup>-</sup> ions adsorb on the passivation film, then attack it, and finally totally remove it. This process is more apt to arise at some flaws and defects [23]. The presence of highly conductive defects on the surface that can explain the observed electrochemical activity of the layer results in its

puncture and localized corrosion [24]. In addition, it is observed that some soluble corrosion products (possibly composed of  $\text{HfBr}_4$ , image D) accumulate on the electrode surface. These soluble corrosion products are mainly generated via the active dissolution of Hf within the pit cavity probably due to the aggressive  $\text{Br}^-$  ions and could appear on the surface from pits by diffusion [25]. SEM observations clearly present the growth of the pitting process, demonstrating the existence of pits on the electrode after anodization in anhydrous *n*-butanol solution containing  $\text{Br}^-$  anion.

**Table 1.** Concentrations of  $\text{Hf}^{4+}$  ions due to pitting in 0.06 M  $\text{Br}^-$  solutions, recorded by ICP-AES, as a function of anodic potential applied ( $> E_{\text{pit}}$ ) at 30 °C. Each tested electrode was applied by the required potential for 5.0 min.

$E_{s,a} / \text{V(Pt)}$	$[\text{Hf}^{4+}] / \text{ppm}$
1.80	0.049
1.85	0.069
1.90	0.17
1.95	0.26
2.00	0.74

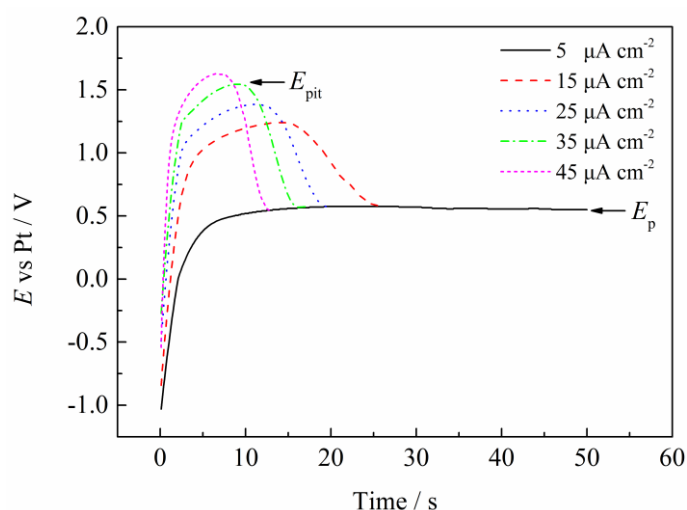
ICP-AES technique of chemical analysis can be utilized to measure  $\text{Hf}^{4+}$  ions dissolved in the corresponding solution at required applied anodic potential ( $> E_{\text{pit}}$ ). Obtained data are collected in Table 1. It is observed that the concentration of  $\text{Hf}^{4+}$  in solution, due to pitting corrosion, enhance with shifting the potential into a positive direction. This confirms polarization results that the pitting of Hf enhances as anodic potential is made more positive.

At  $E_{\text{pit}}$ , the incorporated  $\text{Br}^-$  anions puncture the passive layer at the highly conductive defects, and approach the base metal surface and induce pitting [23, 26]. Nevertheless, Chemistry changes in solution inside pit cavity play a significant role in the propagation and growth of pitting corrosion [27]. As  $\text{Hf}^{4+}$  ions enter solution, giving rise to an increase in the number of  $\text{Br}^-$  ions inside pits through transfer and diffusion, concentration changes of  $\text{Br}^-$  ions in solution tend to take place. The solution within holes in the circumstance becomes more aggressive and facilitates further dissolution of Hf.

Referring again to Fig. 3, it is found that after the potential scan reversal from 3 V (Pt), the anodic current rises still owing to the autocatalytic character of pitting [28]. Subsequently, the anodic current shows to decline linearly, which indicates that an ohmic controlled process is dominating [29]. Eventually, the flyback curve intersects the positive sweeping curve at approximately 0.5 V (Pt), denoted as protection (repassivation) potential ( $E_p$ ) for the Hf electrode. This result indicates that Hf electrode returns again to the passive state. As a whole, a hysteresis loop is evidently formed, a significant character of the pitting corrosion behaviour.

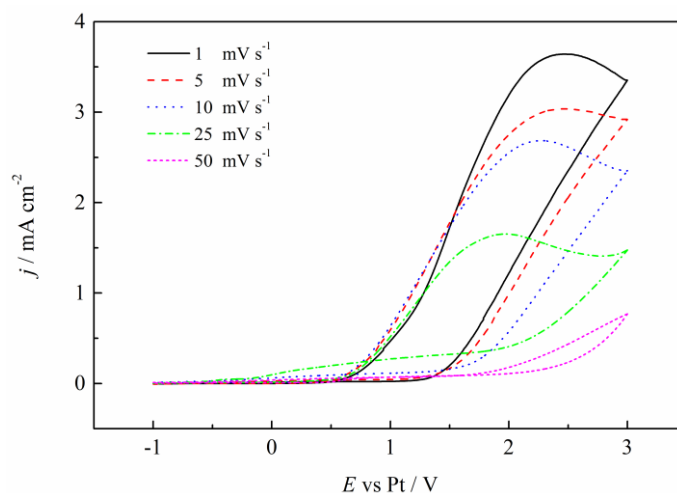
To investigate the growth kinetics of the oxide film formed on Hf surface and its puncture, Hf electrode was applied different constant anodic current density (5-45  $\mu\text{A cm}^{-2}$ ) in 0.06 M  $\text{Et}_4\text{NBr}$  anhydrous *n*-butanol solution at 30 °C, as shown in Fig. 5. These steep linear potential increase with time may be ascribed to the initial appearance and growth of  $\text{HfO}_2$  layer. A maximal potential value can be obtained at a certain time. This maximum is considered as the pitting potential ( $E_{\text{pit}}$ ), which

corresponds to the competition between two processes, namely the growth of porous anodic passivated layer and its puncture. After  $E_{\text{pit}}$ , the potential decays to a nearly constant value, which corresponds to the protection potential ( $E_p$ ). It is clear in galvanostatic curves that  $E_p$  remains nearly a constant, and is independent of time and current [30]. It is important to point out that the values of  $E_p$  observed via cyclic voltammetry in Fig. 2 and Fig. 3 and galvanostatic measurements in Fig. 5 are in good agreements. Moreover, the applied constant current density is found to have a great influence on the values of  $E_{\text{pit}}$ . It is observed in galvanostatic curves that the initial linear slope of the potential versus time enhances with applied anodic current density. This result may be attributed to the rise in the rate of ion transfer through the pre-existing  $\text{HfO}_2$  layer toward the metal/oxide interface, on which the growth of the passivated layer occurs [31]. A rise in the current density is assumed to increase the electric field through the passivated layer, which results in the increase in the rate of ion migration. Therefore, this behaviour may be responsible for the increase of  $E_{\text{pit}}$  with the increase in current density.



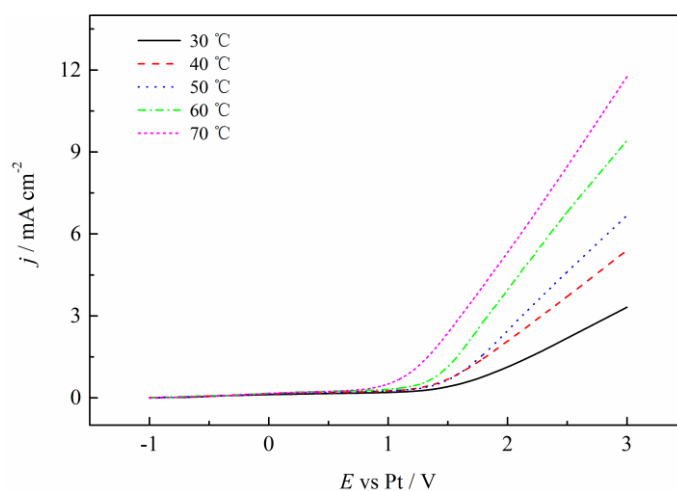
**Figure 5.** Effect of current densities on potential/time transients of Hf in 0.06 M  $\text{Et}_4\text{NBr}$  anhydrous *n*-butanol solution at 30 °C.

Fig. 6 presents cyclic voltammetry curves of Hf in 0.06 M  $\text{Et}_4\text{NBr}$  anhydrous *n*-butanol solution at 30 °C and at various potential scanning rate ( $v$ ). It is clear that increasing scanning rate shifts  $E_{\text{pit}}$  in a positive direction. This result indicates that the anodization time has a direct effect on the pitting potential. This trend could be interpreted in terms of the incubation time ( $t_i$ ) [32] needed for  $\text{Br}^-$  to puncture the barrier film and approach the surface of base metal. The more positive the anodic potential, the shorter will be  $t_i$ , which brings about pitting growth. Thereby, a higher sweep rate decreases the possibility of occurrence of pitting, corresponding to a relative decrease in pit incubation time [32].



**Figure 6.** Effect of potential scanning rates ( $v$ ) on cyclic voltammogram of Hf in 0.06 M  $\text{Et}_4\text{NBr}$  anhydrous  $n$ -butanol solution at 30 °C.

Fig.7 shows the potentiodynamic polarization curve of Hf in 0.06 M  $\text{Et}_4\text{NBr}$  anhydrous  $n$ -butanol solution at a scanning rate of 1  $\text{mV s}^{-1}$  and at various temperatures. With enhancing the solution temperature,  $E_{\text{pit}}$  shifts to negative values. It is possible that a higher temperature enhances the transfer of the soluble corrosion products and reactant into and from the pit cavity. Moreover, enhancing the solution temperature is favorable for the dissolution of the passivating layer [33].



**Figure 7.** Effect of solution temperatures on the potentiodynamic polarization curves of Hf in 0.06 M  $\text{Et}_4\text{NBr}$  anhydrous  $n$ -butanol solution.

Tafel curves of various temperatures are made in order to acquire the apparent activation energy ( $E_a$ ) of the pitting process, as shown in Fig. 8. It is important to note that the shapes and trends of all the curves nearly keep the same, suggesting that the reaction mechanisms do not change with temperature basically. It is known that the corrosion current density ( $j_{\text{corr}}$ ) is a parameter that can evaluate the corrosion property of a material and be calculated by tafel extrapolation.  $E_a$  of Hf in

anhydrous *n*-butanol solution containing 0.06 M Et<sub>4</sub>NBr could be calculated according to the Arrhenius equation [17]:

$$\log j_{corr} = \frac{-E_a}{2.303RT} + A \tag{1}$$

where *A* is a pre-exponential factor, *R* is the universal gas constant and *T* is the absolute temperature. A plot of log *j*<sub>corr</sub> towards *T*<sup>-1</sup> (see Fig. 9) exhibits a straight line (correlation coefficient of 0.978), and the value of *E*<sub>a</sub> obtained from the slope of the straight line is calculated as 49.946 kJ mol<sup>-1</sup>. The value of *E*<sub>a</sub> obtained in anhydrous ethanol system is calculated as 27.074 kJ mol<sup>-1</sup> [20].

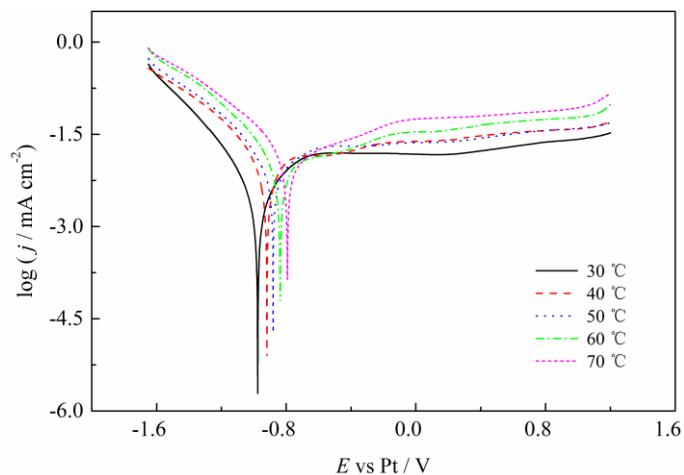


**Figure 8.** Effect of temperatures on tafel curves of Hf in 0.06 M Et<sub>4</sub>NBr anhydrous *n*-butanol solution at a sweep rate of 0.5 mV s<sup>-1</sup>.

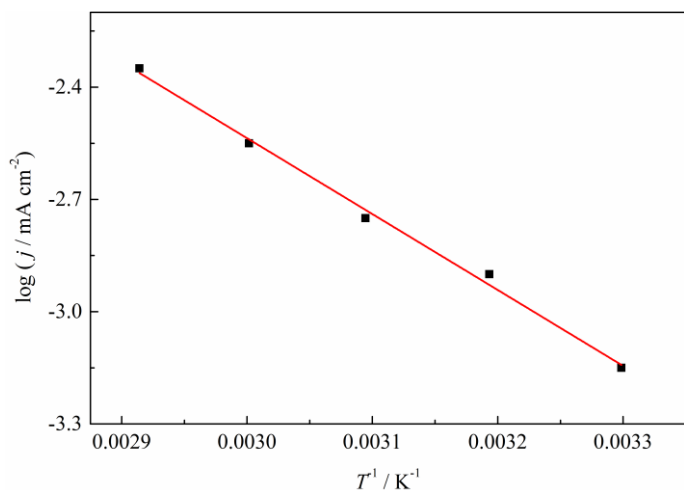


**Figure 9.** Dependence of log *j* on *T*<sup>-1</sup> for Hf in 0.06 M Et<sub>4</sub>NBr anhydrous *n*-butanol solution at a sweep rate of 0.5 mV s<sup>-1</sup>.

Fig. 10 displays the potentiostatic current-time transients of Hf in 0.06 M Et<sub>4</sub>NBr anhydrous *n*-butanol solution at various potentials (*E*<sub>s, a</sub>, before and after *E*<sub>pit</sub>) and at 30 °C with a time of 200 seconds for the experiment. For *E*<sub>s, a</sub> ≤ 1.2 V (Pt) (*E*<sub>s, a</sub> < *E*<sub>pit</sub>, under these conditions), the current

densities( $j$ ) gradually decrease to steady-state values, which suggests that pitting corrosion is not enough to be initiated at a lower potential. The current density decline is considered to be assigned to the growth of  $\text{HfO}_2$  formed on the sample surface. The steady-state current results probably due to the balance competition between the  $\text{HfO}_2$  film formation and its dissolution, which leads to a nearly constant passive layer. However, at  $E_{s,a} = 1.6 \text{ V (Pt)}$  ( $E_{s,a} > E_{\text{pit}}$ , under these conditions),  $j$  initially descends to a minimal value at a certain incubation time ( $t_i$ ), and begins to ascend rapidly due to the puncture of the passivated film caused by the aggressive attack of absorbed  $\text{Br}^-$  ions and the following initiation and propagation of corrosion, which indicates that Hf electrode tend to suffer from pitting corrosion at a higher potential. For  $E_{s,a} \geq 2.0 \text{ V (Pt)}$  ( $E_{s,a} > E_{\text{pit}}$ , under these conditions),  $j$  initially descends to a minimal value at  $t_i$ , and ascends rapidly until a steady-state current is attained. Beyond  $t_i$ , the current density increases rapidly due to propagation and growth of pits. These results may be on the basis that corrosion products precipitate within pit cavities to form a salt film. The corrosion products obstruct the pits, and thus impede the current flow across it. Therefore, a steady-state value was then acquired through competition among the hafnium dissolution, the barrier layer formation, and the corrosion products precipitation. These findings agree well with the SEM observations results.

It is noteworthy that  $t_i$  decreases with enhancing electrode potential. These results indicate that the passivating film has more tendency to be broken down at higher potentials, which are beneficial for the initiation and growth of pitting corrosion. This may be because the adsorption of  $\text{Br}^-$  ions enhances with the increase of anodic potential applied on the electrode surface. Furthermore, it seems that there is a distribution of nucleation sites of different energies that nucleate at distinct potentials [34]. That is to say, the more noble the applied potential, the greater the number of active sites.

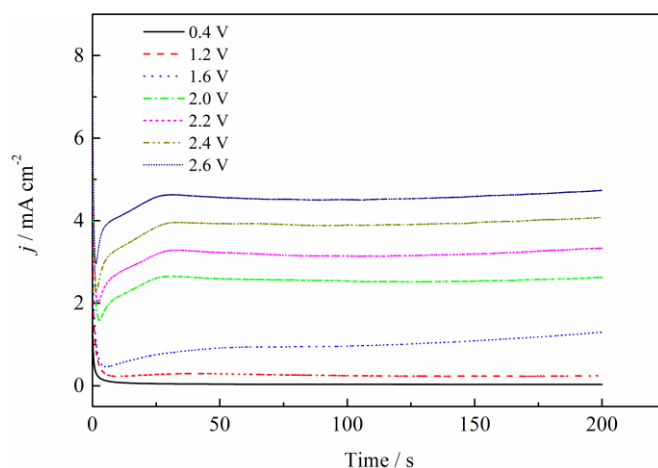


**Figure 10.** Effect of applied potentials on the potentiostatic current-time transients of Hf in 0.06 M  $\text{Et}_4\text{NBr}$  anhydrous  $n$ -butanol solution at 30 °C.

EIS is a very effective technique that can help analyze the various steps involved in an electrochemical reaction by measuring the impedance system response to a small AC potential signal in a wide frequency range [17, 35]. Fig. 11 shows the characteristic nyquist and bode diagrams of Hf in 0.06 M  $\text{Et}_4\text{NBr}$  anhydrous  $n$ -butanol solution at various  $E_{s,a}$  and at 30 °C. It is clearly observed that the impedance declines significantly with enhancing the applied potential from  $-0.4$  to 1.2 V. However,

for the potentials higher than 1.6 V, The impedance decrease evidently slows down and capacitive arcs are substituted by Warburg tails in the low frequency range, which corresponds to the occurrence of corrosive pitting and the formation of a diffusion-controlled process at high applied potentials. This result might be explained in terms of the formation of product salt film caused due to its increasing concentration in the test solution, which impedes the corrosion current across the hole. At the intermediate frequencies, the maximal phase angles in Fig. 11c and d apparently deviate from the values of  $90^\circ$ , and the slopes of magnitude plots in Fig. 11e and f are not the values of  $-1$ . This indicates the deviation from ideal capacitive behavior at intermediate frequencies, which may be associated with the increasing velocity of passivated film dissolution resulted from the enhancing attack by  $\text{Br}^-$  ions [36].

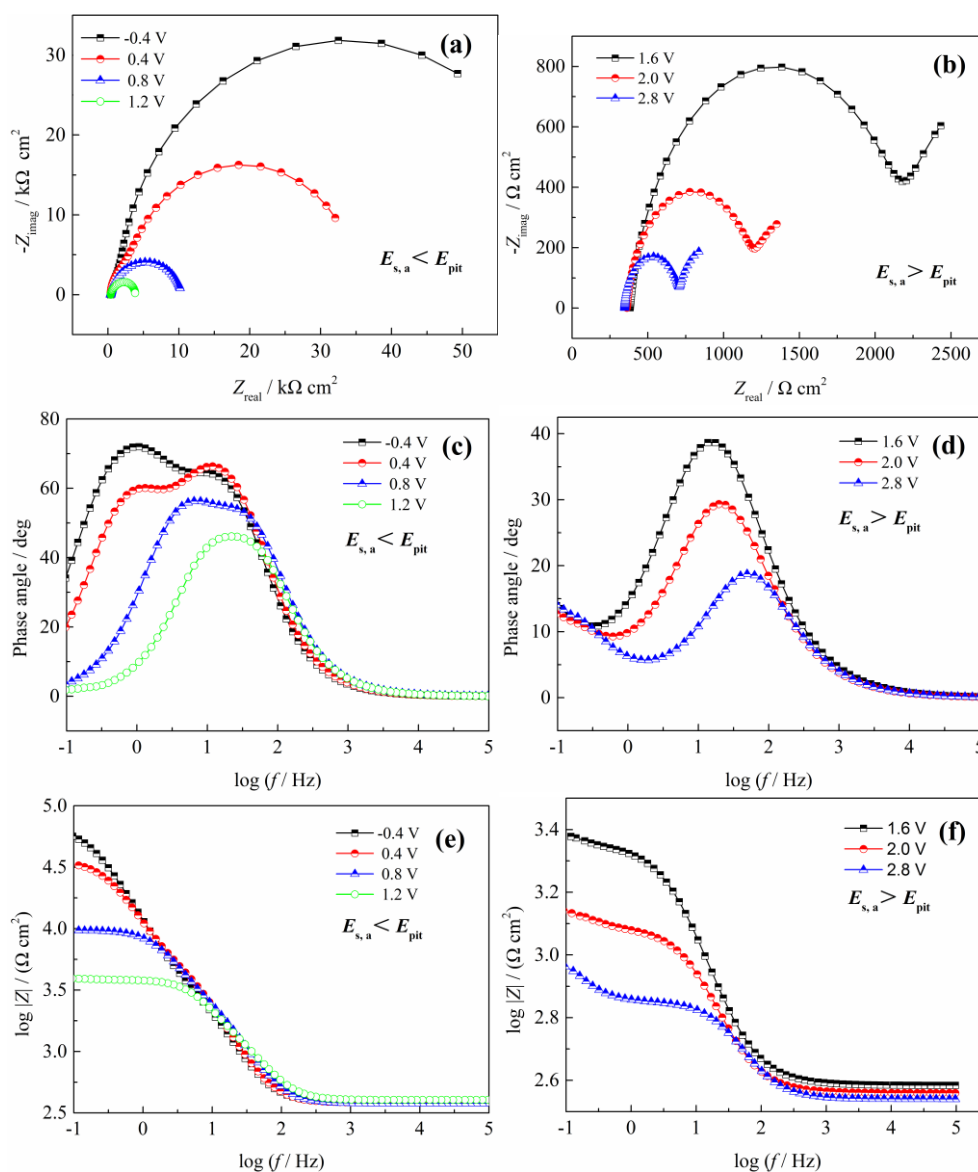


**Figure 11.** Complex plane impedance plots of Hf in anhydrous *n*-butanol containing 0.06 M  $\text{Et}_4\text{NBr}$  at various  $E_{s,a}$  at  $30^\circ\text{C}$ .

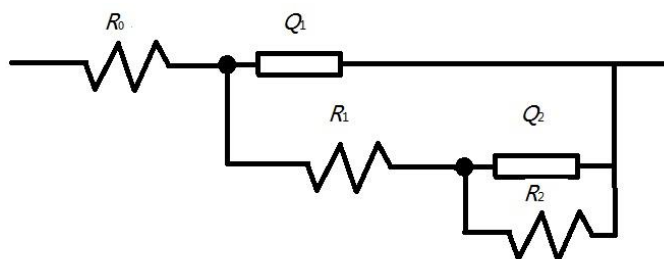


**Figure 12.** Equivalent circuit used to fit the experimental impedance data.

It is important to note that in the nyquist and bode plots from Fig. 11, for all the potentials, two time constants is clearly observed, which can help model an equivalent circuit, as presented in Fig. 12, where  $R_0$  represents the electrolyte resistance,  $R_1$  and  $Q_1$  corresponds to the resistance and capacitance of passivating film, respectively.  $R_2$  represents the charge transfer resistance.  $Q_2$  can be assigned to a constant phase element (CPE) closely correlated with the double layer capacitance. To describe a distribution at a microscopic level, CPE is often adopted through an empirical impedance function [37]:

$$Z_{cpe} = [Q(j\omega)^n]^{-1} \tag{2}$$

in which  $j^2 = -1$  represents an imaginary number,  $\omega$  represents an angular frequency and  $n$  represents a CPE exponent, reflecting the deviation degree from the ideal capacitance. The value of -1 corresponds to the inductance, the value of 0 is in correspondence with a resistor, the value of 0.5 is attributed to a diffusion behaviour and the value of 1 is characteristic of a capacitor. The fitting electrochemical datum are recorded in Table 2. Values of  $R_0$  are nearly constants, while  $R_1$  decreases rapidly with the increase of electrode potentials due to thinning and puncture of the passivating film, further confirming potentiostatic findings that metal dissolution can be facilitated with making potential more positive.

**Table 2.** Electrochemical parameters obtained by fitting EIS measurements.

Potential /V (Pt)	$R_s/$ ( $\Omega$ $\text{cm}^2$ )	$Q_1/$ ( $\Omega^{-1} \text{cm}^{-2} \text{s}^n$ )	$n$	$R_1/$ ( $\Omega \text{cm}^2$ )	$Q_2/$ ( $\Omega^{-1} \text{cm}^{-2} \text{s}^n$ )	$n_1$	$R_2/$ ( $\Omega \text{cm}^2$ )
-0.4	378.1	$5.579 \times 10^{-6}$	0.94	6502	$5.115 \times 10^{-6}$	0.93	58530
0.4	367.3	$5.062 \times 10^{-6}$	0.93	8201	$8.016 \times 10^{-6}$	1	26440
0.8	365.5	$4.109 \times 10^{-6}$	0.93	4109	$8.289 \times 10^{-6}$	1	5484
1.2	397.1	$3.649 \times 10^{-6}$	0.92	1758	$6.696 \times 10^{-6}$	0.88	1680
1.6	383.4	$7.678 \times 10^{-6}$	0.88	1898	$3.977 \times 10^{-4}$	0.46	1357
2.0	362.4	$6.516 \times 10^{-6}$	0.91	875.3	$3.429 \times 10^{-4}$	0.49	530.4
2.8	346.8	$5.001 \times 10^{-6}$	0.94	370.5	$4.112 \times 10^{-4}$	1.06	880.9

Fig. 13 presents potentiostatic current-time transients of the Hf in anhydrous *n*-butanol containing different  $\text{Et}_4\text{NBr}$  concentrations at 30 °C and at 2.5 V (Pt) (this potential lies positive to  $E_{pit}$  under these conditions). It is observed in Fig. 13 that  $j$  initially descends to a minimal value at  $t_i$ , and  $t_i$

becomes shorter with the addition of more number of  $\text{Br}^-$  ions, suggesting that pitting corrosion more tends to occur in a testing solution with higher  $\text{Br}^-$  concentrations. These phenomena are assumed to be associated with the competition between the formation of the soluble passive film and the increase of the number of aggressive  $\text{Br}^-$  ions that dissolve the passivating film. After  $t_i$ , the current density gradually rises steadily due to the puncture of passivated film and the launch of corrosive pitting, which suggests that this potential applied is enough to launch pitting corrosion under these conditions. It is worth noting that as the  $\text{Br}^-$  concentration is enhanced, the corrosion current is increased. This may be interpreted on the basis that the increasing concentration of  $\text{Br}^-$  ion increases the chance for it to adsorb on electrode surface. The  $\text{HfO}_2$  film can be removed especially at some flaws and defects after the adsorption process. When the barrier films are completely removed, the base metal can directly contact the test solution. The higher the bulk  $\text{Br}^-$  ion concentration, the higher will be the local  $\text{Br}^-$  ion concentration that is responsible for initiating pit formation at defect sites and accelerating the bare metal dissolution [20, 38].

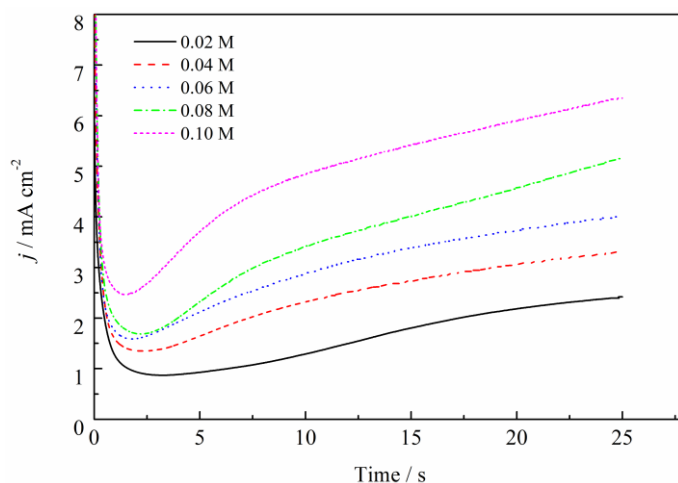


**Figure 13.** Effect of  $\text{Et}_4\text{NBr}$  concentrations on the potentiostatic current-time transients of Hf in anhydrous *n*-butanol at 30 °C and at 2.5 V (Pt) (this potential lies positive to  $E_{\text{pit}}$  under these conditions).

#### 4. CONCLUSIONS

Investigations of the electrochemical behavior for Hf in  $\text{Et}_4\text{NBr}$  *n*-butanol were carried out via open circuit potential measurements, cyclic voltammetry, potentiodynamic anodic polarization, galvanostatic, potentiostatic and impedance techniques, complemented by ICP-AES analysis and SEM examinations. Results reveal that the open circuit potential gets more positive owing to the increased passivity of the passivated layer with increasing immersion time until a steady state value is approached. When a certain anodic potential is applied on the Hf surface, an evident hysteresis loop occurs in cyclic voltammetry, a significant character of the corrosive pitting behaviour. SEM images confirm the existence of pits on the electrode surface owing to the intense attack of  $\text{Br}^-$  ions. In

addition, ICP-AES analysis demonstrates that the pitting propagation rate for Hf increase with enhancing applied anodic potential.

The potentiodynamic polarization curve does not present an activation dissolution section near  $E_{\text{corr}}$  owing to the spontaneous formation of the  $\text{HfO}_2$  layer, followed with severe pitting corrosion as a result of the puncture of the passive film through the intense attack of  $\text{Br}^-$ .  $E_{\text{pit}}$  shifts in a positive direction with increasing potential scan rate, but shifts to more negative values as solution temperature is increased. The apparent activation energy is calculated as  $49.946 \text{ kJ mol}^{-1}$ .

The potentiostatic current–time transients reveal that  $j$  gradually declines to a steady minimal value at a lower fixed potential; however, at a higher fixed potential,  $j$  initially descends to a minimal value and ascends to a steady-state value. The incubation time for passivity puncture decreases with enhancing the electrode potential and  $\text{Br}^-$  concentration. Analysis of the potential/time transients reveals that the applied anodic current density has a great influence on the values of  $E_{\text{pit}}$ . However, the  $E_p$  values are immune to the current density applied. The impedance spectra exhibit two time constants at various potentials applied. The passive film resistance drops rapidly with an increase of electrode potentials owing to thinning and puncture of the passivated film.

#### ACKNOWLEDGEMENTS

We are grateful to the Natural Science Foundation of China (No.51374254) for providing financial support.

#### References

1. M.T. Bohr, R.S. Chau, T. Ghani and K. Mistry, *IEEE Spectrum*, 44 (2007) 29.
2. T. Usui, C.A. Donnelly, M. Logar, R. Sinclair, J. Schoonman and F.B. Prinz, *Acta Materialia*, 61 (2013) 1.
3. I. Karmakov, A. Konova, E. Atanassova and A. Paskaleva, *Appl. Surf. Sci.*, 255 (2009) 9211.
4. F. Zhang, G.X. Liu, A. Liu and F. Shan, *Ceramics International*, 41 (2015) 13218.
5. E. M. Hildebrandt, Oxygen engineered hafnium oxide thin films grown by reactive molecular beam epitaxy, (2012).
6. D.C. Bradley, R. Mehrotra, I. Rothwell and A. Singh, *Alkoxo and aryloxo derivatives of metals*, Academic Press, (2001) San Diego.
7. V.A. Shreider, E.P. Turevskaya, N.I. Koslova and N.Y. Turova, *Inorg. Chim. Acta.*, 53 (1981) 73.
8. S.H. Yang, Y.M. Chen, H.P. Yang, Y.Y. Liu, M.T. Tang and G.Z. Qiu, *T. Nonferr. Metal. Soc.*, 18 (2008) 196.
9. S.H. Yang, Y.N. Cai, H.P. Yang and S.M. Jin, *T. Nonferr. Metal. Soc.*, 19 (2009) 1504.
10. Y.N. Cai, S.H. Yang, S.M. Jin, H.P. Yang, G.F. Hou and J.Y. Xia, *J. Cent. South. Univ. T.*, 18 (2011) 73.
11. E.P. Turevskaya, N.I. Kozlova, N.Y. Turova, A.I. Belokon, D.V. Berdyev, V.G. Kessler and Y.K. Grishin, *Russ. Chem. B+.*, 44 (1995) 734.
12. C. Bartels, J.W. Schultze and U. Stimming, *Electrochim. Acta*, 27 (1982) 129.
13. R.D. Misch, E.S. Fisher, *Journal of the Electrochemical Society Absorbed Electrochem Technol*, 103 (1956) 153.
14. R.D. Misch, W.E. Ruther, *J. Electrochemi. Soc.*, 100 (1953) 531.
15. N. Hackerman, O.B. Cecil, *J. Electrochemi. Soc.*, 101 (1954) 419.
16. M.J. Esplandiu, E.M. Patrito and V.A. Macagno, *J. Electroanal. Chem.*, 353 (1993) 16-176.

17. W.A. Badawy, F.M. Al-Kharafi, *J. Mater. Sci.*, 34 (1999) 2483.
18. S.P. Trasatti, E. Sivieri, *Mater. Chem. Phys.*, 83 (2004) 367.
19. H.P. Yang, S.H. Yang, Y.L. Cai, G.F. Hou and M.T. Tang, *Electrochim. Acta*, 55 (2010) 2829.
20. C.H. Wang, S.H. Yang, Y.M. Chen, B. Wang, J. He and C.B. Tang, *RSC Advances*, 5 (2015) 34580.
21. M. Kutz, *Hand Book of Environmental Degradation of Materials*, Second Edition, William Andrew, (2012) USA.
22. E.E. Stansbury, R.A. Buchanan, *Fundamentals of Electrochemical Corrosion*, ASM International, (2000) USA.
23. A.D. Davydov, *Electrochim. Acta*, 46 (2001) 3777.
24. I. Serebrennikova, H.S. White and I. Serebrennikova, *Electrochem. Solid. ST.*, 4 (2001) B4.
25. S.S.A.E. Rehim, E.E.F. El-Sherbini and M.A. Amin, *J. Electroanal. Chem.*, 560 (2003) 175.
26. S.I. Pyun, S.M. Moon, S.H. Ahn and S.S. Kim, *Corros. Sci.*, 41 (1999) 653.
27. R. Guo, F. Weinberg and D. Tromans, *Corrosion*, 51 (1995).
28. H. Kaesche, *Materials & Corrosion*, 39 (1988) 153.
29. A.G. Muñoz, J.B. Bessone, *Corros. Sci.*, 41 (1999) 1447.
30. Z. Szklarska-Smialowska, *Electrochemical Society Interface*, 19 (1986) 33.
31. I. Montero, M. Fernández and J.M. Albella, *Electrochim. Acta*, 32 (1987) 171.
32. H.D. Duc, P. Tissot, *Corros. Sci.*, 19 (1979) 179.
33. Z. Szklarska-Smialowska, D. Grimes and J. Park, *Corros. Sci.*, 27 (1987) 859.
34. J. Poinot, J. Augustynski, *Electrochim. Acta*, 20 (1975) 747.
35. T. Du, D. Tamboli, Y. Luo and V. Desai, *Appl. Surf. Sci.*, 229 (2004) 167.
36. H.H. Hassan, K. Fahmy, *Int. J. Electrochem. Sci.*, 3 (2008) 29.
37. E. Mccafferty, *Corros. Sci.*, 39 (1997) 243.
38. L.P. Mack, K. Nobe, *Corrosion -Houston Tx-*, 40 (1984) 215.